Effect and mechanism of citric acid on flotation separation of siderite and hematite

Huili Han [1], Wanzhong Yin [1, 2, 3], Jin Yao [1, 2], Dong Li [1]

[1] College of Resources and Civil Engineering, Northeastern University, Shenyang 110819, China

[2] Liaoning key laboratory of mineral processing technology, Shenyang 110819, China

[3] College of Zijin Mining, Fuzhou University, Fuzhou 350180, China

Corresponding author: northeastern2016@foxmail.com (Wanzhong YIN)

Abstract: Heterocoagulation can occur between fine siderite and hematite particles, which would result in the low efficiency of their separation during the flotation process. To date, there have been no mature methods to increase their separation efficiency. In this paper, citric acid was used as a regulator to enhance the slurry dispersion efficiency. Micro-flotation, scanning electron microscopy (SEM) analysis, settling tests, particle size measurements, zeta potential measurements and E-DLVO theoretical calculations were conducted in the investigations. A maximum recovery difference (53.98%) between siderite and hematite in their mixtures flotation was obtained. Settling tests confirmed that citric acid contributed to improving the dispersion degree of the slurry. SEM analysis indicated that citric acid could clean the surface of particles and weaken the coagulation between siderite and hematite, which were in line with the results of particle size measurements. The zeta potential measurements and Extended-Derjaguin-Landau-Verwey-Overbeek (E-DLVO) theoretical calculations indicated that the citric acid could adsorb on the siderite and hematite surfaces and decreased the surface charge, resulting in a visible increase of the repulsion energy between siderite and hematite particles. Therefore, citric acid can be applied to remove the easily-ground carbonate minerals first to improve the flotation performance of hematite in the separation process of carbonate-containing iron ores.

Keywords: siderite, hematite, citric acid, dispersion, flotation, E-DLVO theory

1. Introduction

There is a rich resource of carbonate-containing iron ores in China with a deposit more than 5 billion tons. Generally speaking, siderite and anchorite are the primary carbonate minerals in carbonate-containing iron ores (Luo et al., 2016a, Li et al., 2012; Yang et al., 2013). Rarely existing independently, siderite is often associated with magnetite, limonite, hematite and other iron minerals (Li et al., 2015); thereby carbonate-containing refractory iron ores come into being, such as iron ore processed in Dong Anshan flotation plant in China (Yin et al., 2010; Luo et al., 2017; Luo et al., 2016b). Due to the low hardness, carbonate minerals are easily ground to slime which tends to adhere to or cover on other minerals, resulting in similar surface characteristics and floatability of these minerals. This makes it extremely difficult to separate them even when the valuable minerals have been adequately liberated. Production practice displays that the presence of siderite significantly decreases the iron grade of the concentrate produced by the current reverse anionic flotation process (Zhang et al., 2007; Zhang et al., 2008). To achieve the separation of carbonate-containing refractory iron ores, a two-step flotation process was designed and applied, by which siderite was floated and removed preferentially to diminish the negative effect in the first step and then anionic reverse flotation was used to produce high-quality iron concentrate in the second step (Yin et al., 2010; Zhang et al., 2008; Shao, 2013). However, because of severe coating and heterocoagulation of siderite fines, a portion of hematite and quartz are entrained into the siderite concentrate to be lost in the first flotation step, causing a reduction of the iron

recovery in the second flotation step. To date, the effective separation of siderite from hematite is not yet achieved.

For reducing coating and coagulation of fine particles to improve their flotation performance, it is crucial to clean the particle surfaces and get the particles dispersed effectively before the commencement of the separation process. At present, dispersants have been widely used in flotation for their preferable dispersive effectiveness and convenience in operation (Videla et al., 2016; Oats et al., 2010; Silvestre et al., 2009). So far common organic and inorganic dispersants have been applied to the flotation of coal-slime, fluorite, bauxite, serpentine, galena, pyrite, fine hematite, etc. (Zhu et al., 2015; Luo et al., 2016c; Chen et al., 2014; Silvestre et al., 2009; Wei et al., 2013; Long et al., 2012). Citric acid ($C_6H_8O_7$, H_3L), named 2 - hydroxyl - 1, 2, 3 tricarballylic acid, has three carboxylate groups that can form soluble weakly bound complexes with metal ions. Given the application as a depressant (Zheng and Smith, 1997; Li et al., 2002), the utilization of citric acid as a dispersant was put forward (Luo et al., 2016c). Previous studies have demonstrated that citric acid can alleviate or prevent the coagulation of the bitumen–quartz system and effectively improve particles dispersion (Gan et al., 2009).

In the present work, the interaction effects between siderite and hematite and the dispersion efficiency of citric acid in the separation of these minerals via flotation were investigated by micro-flotation, settling tests, SEM analysis and particle size measurements. The ways that particles are dispersed by citric acid were analyzed using zeta-potential analysis and E-DLVO theoretical calculations.

2.   Materials and methods

2.1. Materials

The pure siderite and hematite sample used in this work were obtained from Anshan City, Liaoning Province, China. They were both carefully hand-picked, crushed, ground, and processed by gravity concentration and magnetic separation. Subsequently, the hematite was wet sieved to obtain a particle size fraction of -74 μm while the -18 μm fraction of siderite was prepared by the elutriation method. The particle size distributions of the siderite sample and the hematite sample show that the siderite and hematite were ground to almost 100% being -18 μm and -74 μm, respectively. The purity of the minerals was examined by X-ray diffraction spectra and chemical composition analysis which indicates that the siderite sample contained about 45.29 wt.-% Fe, and the hematite sample contained about 66.98 wt.-% Fe, that's to say, the mineral samples were of high purity (hematite and siderite > 95%) and they meet the experimental requirement.

Analytical grade citric acid was used as a dispersant of siderite and hematite. Chemical grade sodium oleate was employed as an anionic collector. Corn starch was used as a depressant of hematite, which was dissolved in distilled water at 50°C on a hotplate by the addition of 20 wt.-% sodium hydroxide (NaOH). The pH adjustments were made with dilute solutions of analytical grade NaOH and hydrochloric acid (HCl). Deionized water produced by an automatic adsorption-type ultra-pure water system was employed in all experiments.

2.2. Methods

2.2.1 Flotation tests

The micro flotation experiments were performed in a mechanical agitation flotation machine at 1500 rpm impeller speed. The pulp adopted in single mineral flotation test was prepared by adding 2.0 g of mineral and 20 cm³ of deionized water to the 30 cm³ tank and they were mixed for 1 min. Then the pulp pH was adjusted to the desired value, and the pulp was conditioned for 2 min. Starch and sodium oleate with their desired amount were separately added in sequence and then the pulp was conditioned for 2 min with each reagent. The flotation was conducted for a total of 3 min. The floated and unfloated particles were collected, filtered, and dried. The flotation recovery was calculated based on solid weight distributions between the two products.

The artificial minerals mixture flotation was conducted with an ore sample composed 2 g of -74 μm hematite and 0.4 g of -18 μm siderite. The sample was mixed with 20 cm³ of deionized water in the flotation cell for 1 min. The pulp pH was adjusted and then conditioned for 2 min. Afterwards, the

desired amounts of citric acid, starch and sodium oleate were added respectively in sequence and the system was again conditioned for 2 min with each reagent. Eventually, flotation was performed for 3 min. The products were filtrated, dried, and weighed for assessing the recovery by potassium chromate volumetric analysis. All micro flotation experiments were carried out at room temperature (25 °C).

2.2.2 Scanning electron microscope (SEM) analysis

SEM experiments were carried out through a Hitachi S-3400N scanning electron microscope (Luo et al., 2016c). Prior to examination, the obtained concentrate of the artificially mixed minerals flotation in the presence and the absence of citric acid were prepared and assembled on coded stubs. Afterward, the specimens were placed in a vacuum chamber and sputter-coated with a gold layer, and then examined. Photomicrographs of those particles with the effects of the coating and dispersion were taken. Finally, an Inca energy-dispersive spectrometer attached to the SEM was used to analyze the minerals in the SEM images.

2.2.3 Settling tests

Settling tests are another method to determine the dispersion degree of particle systems. The mixture sample weighing 24 g (4 g of siderite and 20 g of hematite) was added to a beaker containing 200 cm^3 water and was conditioned for 2 min with an electric agitator. The pH value was adjusted and the designated dispersant was added at an appointed dosage, and then the suspension was stirred for 3 min respectively. An extra 1 min settling time for the suspension was provided. The overflow product (W_1) and the underflow fraction (W_2) were collected, filtered, dried, and weighed respectively. The dispersion degree (*DD*) (José et al., 2016; Silvestre et al., 2009) can be calculated as:

$$DD = \frac{W_1}{W_1 + W_2} \times 100\% \tag{1}$$

2.2.4 Particle size measurements

The particle size measurements of the flotation pulp in the absence and presence of citric acid were investigated using a Mastersizer 2000 instrument (Malvern Instruments, UK). The mixture sample weighing 2.4 g (0.4 g of siderite and 2.0 g of hematite) was added to the 30 cm^3 flotation tank and then mixed for 1 min. The pH value was adjusted and the designated dispersant was added at an appointed dosage. Further, the pulp was conditioned for 3 min. Finally, some of the mixture was sucked out using a wide-diameter pipette and added to a beaker filled with 1 dm^3 of deionized water. The particles were then stirred using an overhead impeller at 3000 rpm to maintain the particles in dispersion during the measurement (Liang et al., 2018). The size distribution of the particles was determined using the standard instrument software (Malvern Instruments, UK).

2.2.5 Zeta potential measurements

Zeta potentials of samples were measured with a Malvern Instruments Nano ZS-90 zeta potential analyzer (Yao et al., 2016). The mineral particles (pure siderite or hematite) were finely ground to -0.005 mm in an agate mortar. A suspension containing 0.04 wt.-% solids (20 mg of minerals and 50 cm^3 of distilled water) in 1×10^{-3} mol/dm^3 KCl solution was agitated for 15 min with a mechanical agitator so that the particles were fully dispersed. The pH values of the suspensions were adjusted. At a constant temperature of 25°C, the zeta potentials of the mineral samples surfaces were measured in distilled water and then were measured again in the solution of citric acid at its given concentration. To assess the accuracy of the measurements, the zeta potential of at least three independent suspensions was evaluated, and the measurement tolerance was ±2 mV.

2.2.6 Contact angle measurements

The contact angle values of the hematite and siderite surfaces were determined by sessile drop experiments and were analyzed by a JC2000A contact angle goniometer. The pure mineral samples were

polished and cut to a proper size approximately 2×1.5×1 cm, subsequently washed thoroughly with distilled water. Afterwards, half of the cleaned samples were immersed in distilled water at the corresponding pH value and the rest cleaned samples were immersed in the solution of citric acid at its predetermined concentration and pH value for 10 min, and then dried at room temperature in vacuum. A liquid drop was introduced onto the substrate by a microsyringe after the sample was located in a rectangular glass chamber. The needle was adjusted so that its tip was just above the sample surface. The measurements were conducted carefully for different liquid drops of 3-4 mm base diameter and repeated three times at least under each condition for the acquisition of average value with an accuracy of ±1∘(Gu et al., 2016). After acquiring the side view of the sessile drop, the half-angle algorithm was applied to calculate the contact angle values.

2.2.7 E-DLVO theoretical calculations

Calculations of the interaction energies between siderite and hematite particles based on the E-DLVO theory are employed to quantitatively evaluate the dispersing effect of citric acid. According to the E-DLVO theory, the total interaction energy between particles mainly comprises the following components: Vander Waals interaction, electrostatic interaction, and hydrophobic or hydration interaction (Li et al., 2017). The total interaction energy (Hu and Dai, 2003) is given by

$$V_{TED} = V_W + V_E + V_H \tag{2}$$

where V_{TED}, V_W, V_E and V_H are the total interaction energy, Van der Waals energy, electrostatic interaction energy, and hydrophobic or hydration interaction, respectively. The Van der Waals energy of a spherical particle and a platy particle (for fine and coarse particles) (Verwey and Overbeek, 1955; Schenkel and Kitchener, 1960) can be calculated as:

$$V_W = -\frac{A_{132}R_1}{6H} \tag{3}$$

$$A_{132} \approx (\sqrt{A_{11}} - \sqrt{A_{33}})(\sqrt{A_{22}} - \sqrt{A_{33}}) \tag{4}$$

where H is the distance between two mineral particles; R is the radius of spherical particles; A_{11} and A_{22} are the Hamaker constants of mineral 1 and mineral 2 separately; A_{33} is the Hamaker constant of water in vacuum; A_{132} is the effective Hamaker constant of mineral 1 and 2 in medium 3. The electrostatic interaction energy of different minerals (Pugh and Kitchener, 1971; Hogg et al., 1966) is usually determined by the following equation:

$$V_E = \frac{\pi \varepsilon_a R_1 R_2}{R_1 + R_2} (\varphi_{01}^2 + \varphi_{02}^2)[\frac{2\varphi_{01}\varphi_{02}}{\varphi_{01}^2 + \varphi_{02}^2} p + q] \tag{5}$$

$$p = \ln\left(\frac{1 + \exp(-\kappa H)}{1 - \exp(-\kappa H)}\right) \tag{6}$$

$$q = \ln[1 - \exp(-2\kappa H] \tag{7}$$

Here κ is the Debye length which is 0.104 nm^{-1}; $\varepsilon_a = \varepsilon_0 \varepsilon_r$, ε_0, and ε_r are the permittivities of vacuum and of the solution (water is 78.5 C^{2}J^{-1}m^{-1}), respectively and $\varepsilon_a = 6.95 \times 10^{-10}$ C^{-2}J^{-1}m^{-1}; φ_{01} and φ_{02} are the surface potentials of siderite and hematite, respectively. The polar interfacial interaction energy of a spherical particle and a platy particle (Israelachvili and Pashley, 1982; Claesson et al., 1986) is expressed as follows:

$$V_H = 2\pi R_1 h_0 V_H^0 \exp\left(\frac{H_0 - H}{h_0}\right) \tag{8}$$

where h_0 is the decay length, and its reasonable value seems to be about 1nm (Van Oss, 2006); H_0 is the minimum equilibrium contact distance between particles and $H_0 = 0.15$nm (Van Oss, Giese, and Costanzo, 1990). V_H^0 is the acid-base free energy per unit area between the surfaces, and it can be calculated by the following equation:

$$V_H^0 = 2[\sqrt{\gamma_3^+}(\sqrt{\gamma_1^-} + \sqrt{\gamma_2^-} - \sqrt{\gamma_3^-}) + \sqrt{\gamma_3^-}(\sqrt{\gamma_1^+} + \sqrt{\gamma_2^+} - \sqrt{\gamma_3^+}) - \sqrt{\gamma_1^+ \gamma_2^-} - \sqrt{\gamma_1^- \gamma_2^+}] \tag{9}$$

where γ_1^+, γ_2^+, γ_3^+, γ_1^-, γ_2^-, γ_3^- are the parameters of the polar components of the surface tension of material 1, material 2 and medium 3, donating an electron or accepting a proton. γ_1^-, γ_2^+, γ_2^- can be calculated as (VAN OSS et al., 1990; VAN OSS et al., 1987; VAN OSS et al.,1988; VAN OSS et al., 1987; VAN OSS et al., 1989)：

$$(1+\cos\theta)\gamma_L = 2(\sqrt{\gamma_S^d \gamma_L^d} + \sqrt{\gamma_S^+ \gamma_L^-} + \sqrt{\gamma_S^- \gamma_L^-}) \tag{10}$$

where γ_L, γ_L^d, γ_L^+, γ_L^- and γ_S^d, γ_S^+, γ_S^- are the parameters of the polar components of the surface tension of the liquid phase and the solid phase and θ is the contact angle between the liquid and the solid. Because most oxidized minerals have a monopolar surface, for which, $\gamma_S^+ \approx 0$ (Qiu et al., 1993), equation (10) can be simplified as:

$$(1+\cos\theta)\gamma_L = 2(\sqrt{\gamma_S^d \gamma_L^d} + \sqrt{\gamma_S^- \gamma_L^-}) \tag{11}$$

Thus, by contact angle measurements with only two different liquids (both must be polar) with known γ_L^d, γ_L^+ and γ_L^- values and by using equation (11) twice, the values for γ_S^d and γ_S^- of siderite and hematite can be determined.

The Hamaker constant can be determined by γ_s^d using the following equation (Bergström, 1997):

$$A = 2.05\times10^{-21}\gamma_s^d \tag{12}$$

3.   Results and discussion

3.1.   The interaction effects between siderite and hematite

The interaction of -18 μm siderite and -74 μm hematite in the flotation process was investigated. Firstly, Fig. 1(a) shows the siderite flotation recovery in the single mineral flotation and the mixtures flotation of siderite-hematite as a function of the pH value. The recovery of siderite in the flotation of mixtures increased steadily with the increase of pH value from approximately 5.4 to 9.0 and reached a maximum at about pH 9.0, and then decreased sharply with continually increasing pH from 9.0 to 11.2. There is a similar tendency in the recovery of siderite in single mineral flotation with increasing pH besides its optimal recovery is attained at about pH 10.0. As can be seen, siderite recovery in the artificial mixture flotation is about 20% higher than that in the single mineral flotation in pH range from 5.4 to about 9.6. In contrast, siderite recovery in the artificial mixture flotation is lower than that in the single mineral flotation in pH range from 9.6 to 11.2. This result indicates that the presence of hematite elevates the flotation recovery of siderite in pH range from 5.4 to about 9.6 and then brings it down in pH range from 9.6 to 11.2.

Fig. 1(b) presents the hematite flotation recovery in the single mineral flotation and the mixtures flotation as a function of pH value. The recovery of hematite in the mixed minerals flotation improved up from 19.46% to 59.04% with the increase of pH value from 5.4 to 7.1 and then was close to leveling off in pH range from 7.1 to 9.0, afterward decreased obviously to about 10% and finally remained steady with increasing pH value to 11.2. The hematite recovery in the single mineral flotation increased firstly, then declined and finally stabilized with the increase of pH value from 5.0 to 11.0, and got the high point of 40% at pH 6.6. The result indicates that the presence of siderite significantly influenced the flotation of hematite. Compared with the single mineral flotation of hematite, the presence of siderite leads to an obvious improvement of the hematite recovery in the pH range from about 5.0 to 10.0; this is to say, the floatability of hematite is improved owing to siderite.

Fig. 1(c) shows the recovery of siderite and hematite in the single mineral flotation as a function of pH value. The recovery of siderite in the single mineral flotation was higher than that of hematite over the whole investigated pH range, suggesting that the inhibitory effect of corn starch on hematite was stronger than that on siderite, which is consistent with the literature (Yin et al., 2016; Luo et al., 2014). Obviously, it is easy to separate hematite from siderite in pH range from 8.1 to about 11.0 especially at pH 10.0 when there is no other coexisting mineral.

The recovery of siderite and hematite in the mixtures flotation as a function of pH value is presented in Fig. 1(d). It can be observed from Fig. 1(d) that the variation trends of these two recovery curves were nearly the same. It is important that the differential values between the recoveries of siderite and hematite in the mixtures flotation were smaller than that in the single mineral flotation (see Fig. 1(c)),

which indicates that it becomes difficult to separate hematite from siderite in the flotation of artificially mixed minerals.

In order to reduce the recovery of hematite in siderite concentrate, citric acid was employed in their flotation separation.
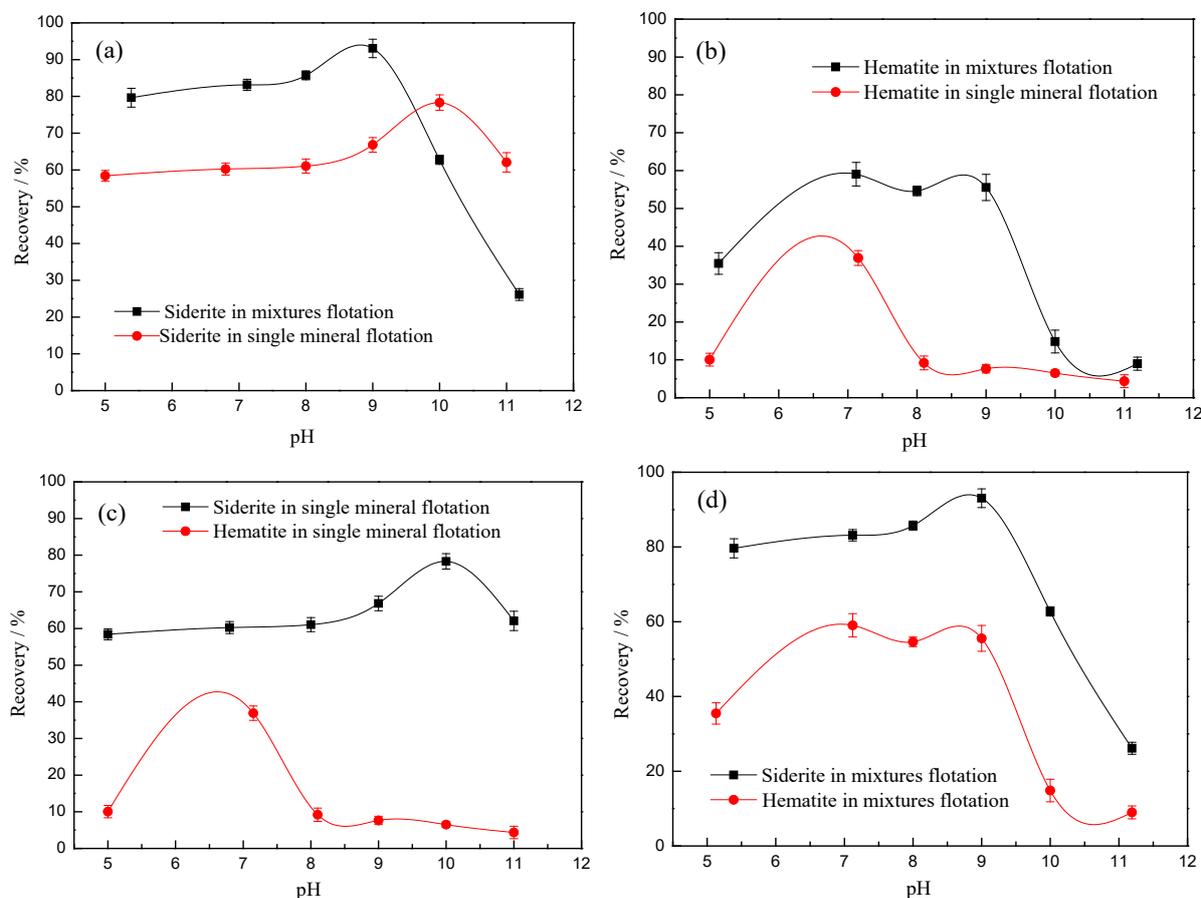
Fig. 1. Recovery as a function of pH value: siderite (a) and hematite (b) in the single mineral flotation and the mixtures flotation; siderite and hematite in the single mineral flotation (c) and the mixtures flotation (d) (sodium oleate concentration: 150 mg/dm³; corn starch concentration: 20 mg/dm³, the single mineral sample: 2.0 g of -18 μm siderite or -74 μm hematite; the mixtures sample: 0.4 g of -18 μm siderite and 2.0 g of -74 μm hematite)

3.2. Effect of citric acid on separation of siderite from hematite

The recoveries of siderite and hematite as a function of citric acid concentration in their mixture flotation at pH=9.0 are presented in Fig. 2. Compared with the absence of citric acid (0 mg/dm³), its addition reduced both recoveries of siderite and hematite whereas the degree of reduction in hematite recovery was larger than that in siderite recovery. Particularly, the largest gap between their recoveries (53.98%) occurred when the citric acid concentration was 20 mg/dm³, and the recoveries of siderite and hematite were 82.99% and 29.01% at that point, respectively. The decrease of the hematite recovery indicates that hematite was depressed effectively by starch thereby was prevented from entering into siderite concentrate because the dispersion of particles was improved by adding citric acid.

SEM analysis of mineral particles in the foam of the mixtures flotation was conducted, and the SEM micrograph is presented in Fig. 3(a). As evident in Fig. 3(a), numerous siderite fines adhered to the coarse hematite particles. After coated with siderite fines, hematite particle surface has the similar properties as siderite particles. Thus, the inhibitory effect of corn starch on hematite is weakened due to the inhibition effect on siderite is slighter than that on hematite, and then the floatability of hematite is elevated. Besides, the coating of siderite on hematite surface results in a reduction of the active points on the hematite surface for the adsorption of starch, thus decreasing the inhibitory effect (Luo, 2014).

Accordingly, an appreciable increase in the hematite recovery was caused, which promotes the inclusion of hematite particles into the siderite concentrate during their flotation separation.
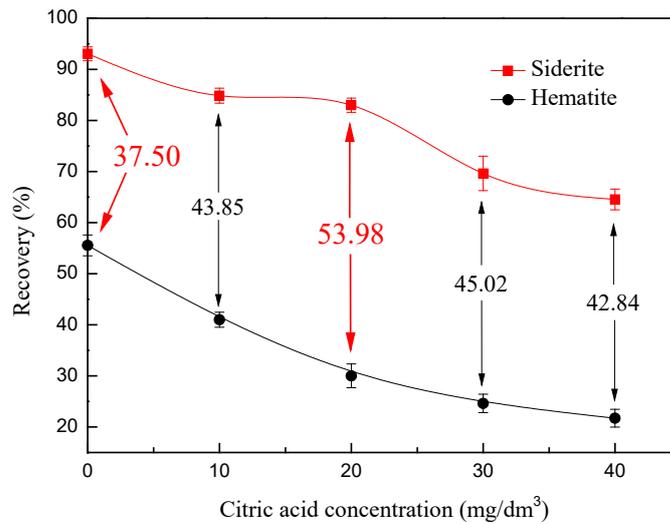
Fig. 2. Recoveries of siderite and hematite in the mixtures flotation as a function of citric acid concentration (sodium oleate concentration: 150 mg/dm³; corn starch concentration: 20 mg/dm³; pH: 9.0)

Coarse hematite particles whose floatability was elevated can serve as carriers for fine siderite particles (Li et al., 2017). The flotation efficiency for the siderite particles on the coarser hematite particles is higher due to a more appropriate particle size for flotation. Thereby the siderite recovery in the mixtures flotation was increased (in Fig. 1(a)).

The SEM micrograph of mineral particles in the foam product with 20 mg/dm³ of citric acid was presented in Fig. 3(b) to verify the dispersing effect of citric acid. As can be seen, the surface of hematite particle has been much cleaner though there are a few siderite fines adhering on the surface of the hematite particle, proving that the coating and aggregation have been exactly weakened by citric acid.
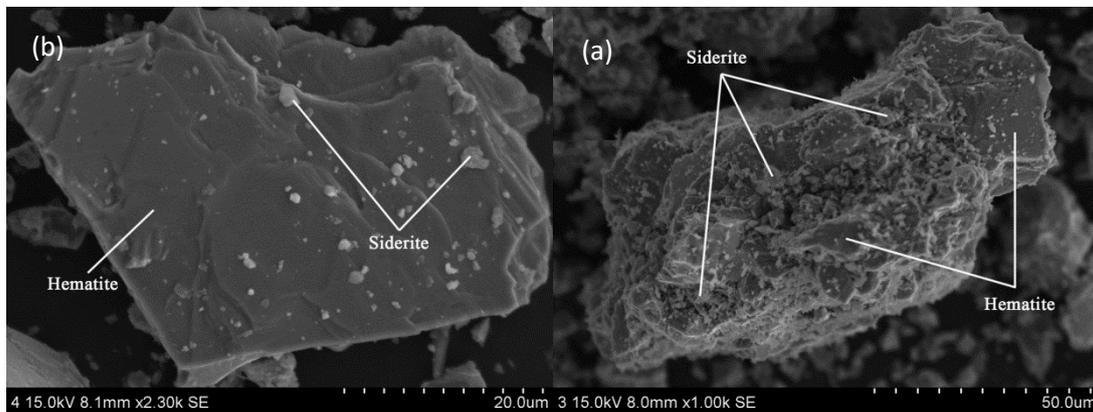
Fig. 3. SEM images of mineral particles in the foam product of the mixtures flotation: (a) without citric acid; (b) with citric acid at a concentration of 20 mg/dm³

The dispersion degrees (*DD*) of the siderite and hematite mixtures as a function of citric acid concentration are presented in Fig. 4. When the citric acid concentration is increased from 0 to 20 mg/dm³, the *DD* of the mixtures raised from about 7.2% up to 11.9%. At higher citric acid concentrations, the increase in the *DD* of the mixtures was much slower. The settling tests indicated that citric acid has a great dispersing effect on mineral particles in the slurry, which is in good agreement with the SEM analysis.

For the mixture of siderite (-18 μm) and hematite (-74 μm) treated with or without citric acid at a concentration of 20 mg/dm³, the size distributions of particles in the pulp were obtained using a

Malvern Mastersizer instrument, as shown in Fig. 5. Compared with the size distribution of particles in the absence of citric acid, the amount of fine particles with the size of -48 μm (especially -18 μm) in the mixture increased while the amount of coarse particles with the size of +48 μm decreased after adding citric acid. The decrease in the size of some aggregate confirmed that the particles were indeed dispersed. Comparison of this result with the SEM analysis showed good agreement: citric acid can clean the surface of particles to get them dispersed and reduce the coating and aggregation, consistent with an increasing dispersion degree of the pulp in the settling tests
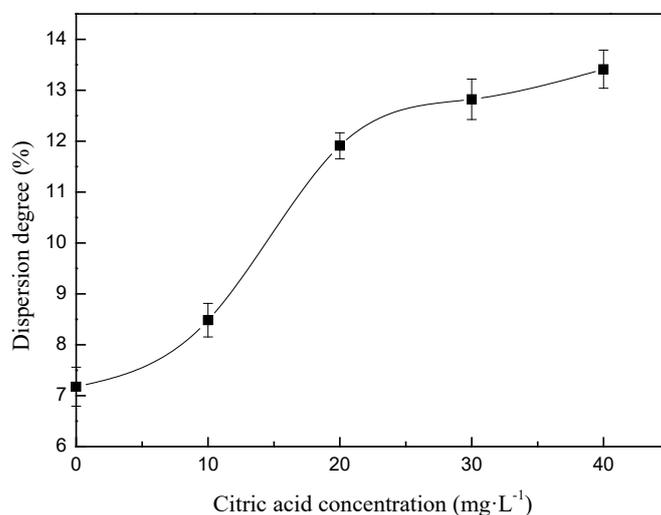
Fig. 4. Dispersion degree of the mixture (siderite-hematite) as a function of citric acid concentration
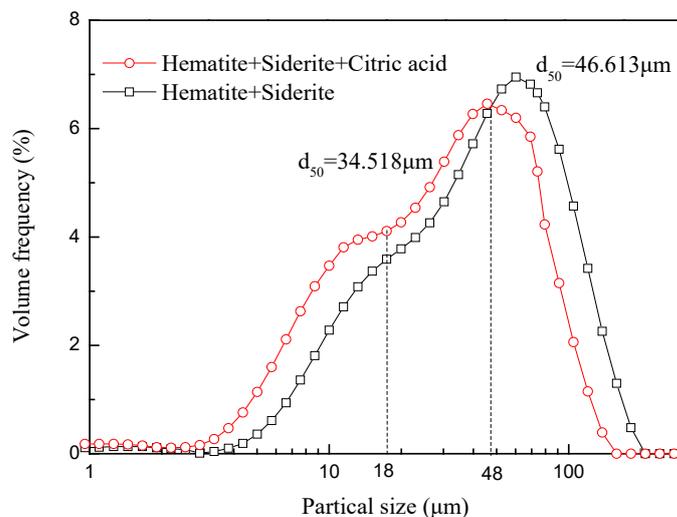
Fig. 5. The volume size distributions of the particles in the pulp (0.4 g of -18 μm siderite and 2.0 g of -74 μm hematite)

3.3. Mechanism of citric acid to disperse siderite and hematite

The zeta potentials of siderite and hematite as a function of pH value in the presence and absence of citric acid are depicted in Fig. 6. Compared to the absence of citric acid situation, the zeta potential of both siderite and hematite evidently decreased over the whole investigated pH range in the presence of citric acid at 20 mg/dm^3. The species distribution diagram of citric acid at its concentration of 1.04×10^{-4} mol/dm^3 (20 mg/dm^3) as a function of pH value is presented in Fig. 7. According to the results in Figs. 6 and 7, it can be acknowledged that citric acid absorbs onto the siderite and hematite surface as H_2L^- (3.1≤pH＜4.9), HL^{2-} (4.9≤pH＜6.4) and L^{3-} (pH≥6.4), decreasing the zeta potentials of siderite and hematite surfaces in corresponding pH values and increasing the electrical double-layer repulsion

between particles (Luo et al., 2016c). Consequently, the coagulation is reduced and the dispersion of the system is promoted.

Previous studies indicated that no chemical adsorption occurs when citric acid adsorbs onto the iron minerals surface (Luo, 2014). Because the siderite or hematite surfaces are negatively charged at pH 9.0 (Fig. 6), there is no electrical double-layer adsorption between minerals and citric acid. It is likely that citric acid adsorbs physically onto the minerals by hydrogen bonds which can be formed via O–H$_3$L and OH–mineral surfaces in an alkaline environment (Luo et al., 2016c).
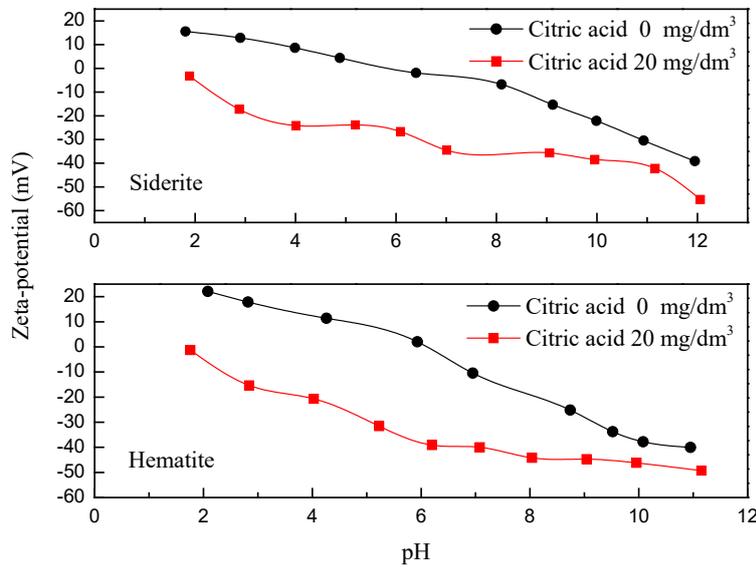
Fig. 6. Zeta potentials of siderite and hematite as a function of pH value in the presence and absence of citric acid
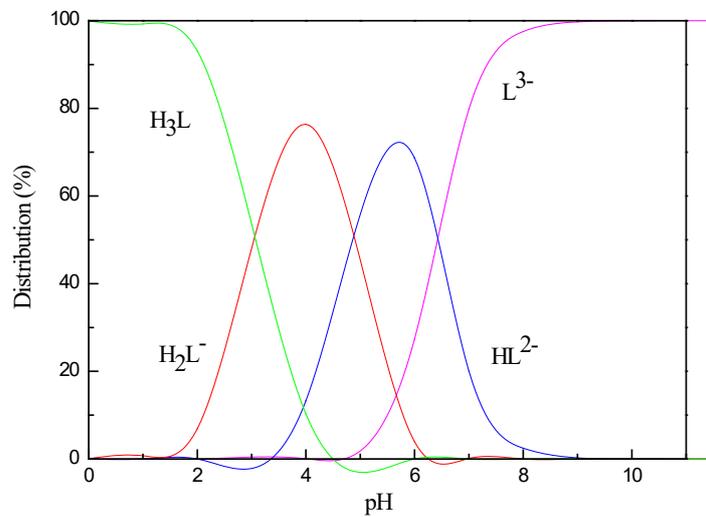
Fig. 7. Species distribution diagram of citric acid 1.04×10^{-4} mol/dm³ as a function of pH value (Hu et al., 1998)

Static contact angles are also measured in this study to acquire the correlated parameters for the E-DLVO theoretical calculation. Table 1 gives the average contact angle values at the siderite and hematite surfaces in the presence and absence of citric acid (20 mg/dm³) in distilled water and glycerin at pH 9.0. Table 2 shows the known values of the surface energy components of water and glycerin. The surface potentials, Hamaker constants and values of components of the surface energy of siderite and hematite are calculated on the basis of Eqs. (11) - (12) and presented in Table 3.

Based on Eqs. (2) - (12), the total interaction energy between siderite and hematite particles in the presence and absence of citric acid at pH 9.0 are calculated and presented in Fig. 8. It can be observed that the addition of citric acid could increase the energy barrier and the repulsion energy between

siderite and hematite obviously, which makes the heterocoagulation more difficult. It can be concluded that citric acid can contribute to a greater dispersion of the pulp by enlarging the total E-DLVO energy between particles.

Table 1. Average contact angles with and without citric acid in distilled water and glycerin (∘)

Minerals	Siderite		Hematite	
	No citric acid	With citric acid	No citric acid	With citric acid
Water	66	40	38	21
Glycerin	80	95	91	75

Table 2. Surface tension parameters of water and glycerin

Species	γ_L (mJ/m²)	γ_L^d (mJ/m²)	γ_L^+ (mJ/m²)	γ_L^- (mJ/m²)
Water	72.8	21.8	25.5	25.5
Glycerin	64	34	3.92	57.4

Table 3. Surface potentials, Hamaker constants and values of components of the surface energy of siderite and hematite

Species	Siderite				Hematite			
	φ_{01} (mV)	A (10^-20 J)	γ_s^d (mJ/m²)	γ_s^- (mJ/m²)	φ_{02} (mV)	A (10^-20 J)	γ_s^d (mJ/m²)	γ_s^- (mJ/m²)
No citric acid	-14.2	3.92	19.11	37.17	-27.9	0.45	2.19	132.66
With citric acid	-35.0	0.21	1.00	139.31	-44.5	2.06	10.06	121.07
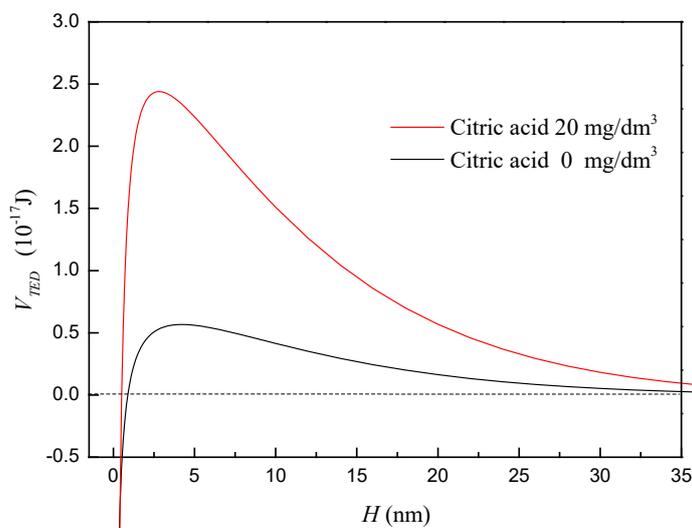
Fig. 8. Total interaction energy between siderite and hematite particles in the presence and absence of citric acid

According to the results obtained above, the dispersion effect and mechanism of citric acid in the flotation separation of siderite and hematite can be explicitly elucidated by the schematic diagram in Fig. 9. Fig. 9(a) illustrates that many fine siderite particles with strong attraction severely adhered on the surface of coarse hematite particles which were brought onto the air bubble to float into the siderite concentration during the flotation without citric acid. By comparison, when citric acid was added into the pulp and adsorbed on the surface of minerals, their surface properties were improved and the repulsion between them was elevated. Thus, some undesirable behaviors such as coating and aggregation are avoided. As Fig. 9(b) displays, a good dispersion of particles is achieved by adding citric acid, and siderite can be separated from hematite effectively.

(a) Heterocoagulation without citric acid：● Hematite ● Siderite

(b) Dispersion with citric acid：⊖ Citric acid
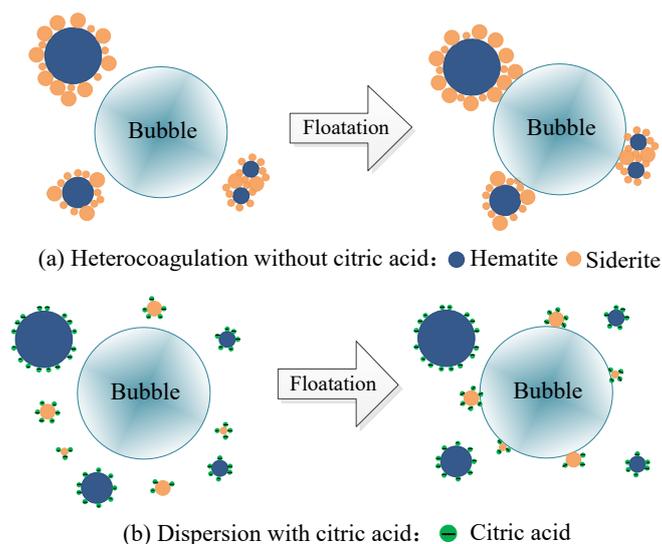
Fig. 9. Eliminating coating and coagulation effects of particles in flotation due to the dispersing effect of citric acid

4. Conclusions

The flotation separation of siderite from hematite has been conducted. In this study, the recoveries of siderite and hematite in the mixtures flotation were higher than that in their single mineral flotation, which was obviously due to the heterocoagulation between siderite and hematite, resulting in the low separation efficiency of siderite from hematite. Citric acid, which was used as a regulator, increased the separation efficiency between siderite and hematite, and a maximum difference between their recoveries of 53.98% was obtained. SEM analysis and settling tests suggested that citric acid could clean the surface of particles, weaken the coagulation between siderite and hematite, and enhance the dispersion degree of the slurry. In addition, the decrease of aggregate size also confirmed that the dispersion between particles was improved by citric acid. The zeta potential measurements and E-DLVO theory calculations demonstrated that the citric acid could adsorb onto the surfaces of siderite and hematite, resulting in decreasing the surface charge and visibly enlarging the total repulsion energy between siderite and hematite particles, which might explain the dispersion mechanism of citric acid in flotation separation of siderite from hematite. This study is significant for improving the flotation performance of iron ores that contain carbonate minerals by removing the carbonate minerals preferentially.

Acknowledgments

References

BERGSTRÖM L., 1997. *Hamaker constants of inorganic materials*, Adv. Colloid Interface Sci., 70, 125-169.

CHEN, M., NIU, F.S., BAI, L.M., 2014. *Dispersion behaviors research of three dispersants on the micro-fine hematite and quartz*, China Min. Mag., 23, 116-118.

CLAESSON, P.M., BLOM, C.E., HERDER, P.C., NINHAM, B.W., 1986. *Interactions between water-stable hydrophobic Langmuir-Blodgett monolayers on mica*, J. Colloid Interface Sci., 114, 234-242.

GAN, W.B., CROZIER, B., LIU, Q., 2009. *Effect of citric acid on inhibiting hexadecane-quartz coagulation in aqueous solutions containing Ca^{2+}, Mg^{2+} and Fe^{3+} ions*, Int. J. Miner. Process., 92, 84-91.

GU, H.Y., WANG, C., GONG, S.J., MEI, Y., LI, H., MA, W.M., 2016. *Investigation on contact angle measurement methods and wettability transition of porous surfaces*, Surf. Coat. Technol., 292, 72-77.

HPGG, R., HEALY, T.W., FUERSTENAU, D.W., 1966. *Mutual coagulation of colloidal dispersions,* Trans. Faraday Soc., 62, 1638-1651.

HU, Y.H., SUN, W., JIANG, Y.R., XU, J., 1998. *Study on the inhibitory effect and mechanism of citric acid in the flotation separation of scheelite and fluorite,* Metall. Ore Dressing Abroad, 5, 27-29.

HU. Y., DAI, J., 2003, *Hydrophobic aggregation of alumina in surfactant solution,* Miner. Eng., 16, 1167-1172.

ISRAELACHVILI, J., PASHLEY, R., 1982. *The hydrophobic interaction is long range, decaying exponentially with distance*, Nat. 300, 341-342.

JOSÉ, F. D. S., IMBELLONI, A. M., NOGUEIRA, F. C., PEREIRA, C. A., 2016. *Nickel Ore Dispersion Evaluation and Consequences in Flotation Process*, Metall. Mater. Trans. B., 47, 899-904.

LI, D., YIN, W.Z., LIU, Q., CAO, S.H., SUN, Q.Y., ZHAO, C., Yao, J., 2017. *Interactions between fine and coarse hematite particles in aqueous suspension and their implications for flotation*, Miner. Eng., 114, 74-81.

LI, L.X., YIN, W.Z., WANG, Y.B., TAO, S.J., 2012. *Effect of siderite on flotation separation of martite and quartz*, J. Cent. South Univ., 33, 431-434.

LI, Y., LEI, D.S., LU, W., XU, S., 2002. *Effects of citric acid on separation of sillimanite from quartz*, Chin. J. Nonferrous Met., 12, 979-982.

LI, Y.J., YANG, G., ZHAO, R.C., HAN, Y.X., YUAN, S., 2015. *Feature of refractory iron ore containing siderite and its research trends of beneficiation technology*, Multipurpose Util. Miner. Resour., 2, 12-25.

LIANG, G.J., NGUYEN, A.V., CHEN, W.M., NGUYEN, T.A.H., BIGGS, S., 2018. *Interaction forces between goethite and polymeric flocculants and their effect on the flocculation of fine goethite particles*, Chem. Eng. J., 334, 1034-1045.

LONG, T., FENG, Q.M., LU, Y.P., 2014. *Dispersive mechanism of sodium hexametaphosphate on flotation of copper-nickel sulphide*, Chin. J. Nonferrous Met., 22, 1763-1769.

LU, Y.P., LONG, T., FENG, Q.M., OU, L.M., ZHANG, G.F., 2009. *Flotation and its mechanism of fine serpentine*, Chin. J. Nonferrous Met., 19, 1493-1497.

LUO, X.M., 2014. *Research on Interactive Effect among Minerals in Flotation System of Carbonate -containing Iron Ore*, Northeastern University, Shenyang, China.

LUO, X.M., WANG, Y.F., MA, M.Z., SONG, S.X., ZHANG, Y., DENG, J.S., LIU, J., 2017. *Role of dissolved mineral species in quartz flotation and siderite solubility simulation,* Physicochem. Probl. Miner. Process., 53, 1241-1254.

LUO, X.M., WANG, Y.F., WEN, S.M., MA, M.Z., SUN, C.Y., YIN, W.Z., MA, Y.Q., 2016a. *Effect of carbonate minerals on quartz flotation behavior under conditions of reverse anionic flotation of iron ores*, Int. J. Miner. Process., 152, 1-6.

LUO, X.M., YIN, W.Z., WANG, Y.F., SUN, C.Y., MA, Y.Q., LIU, J., 2016b. *Effect and Mechanism of Siderite on Reverse Anionic Flotation of Quartz from Hematite*, J. Cent. South Univ., 23. 52-58.

LUO, X.M., YIN, W.Z., SUN, C.Y., WANG, N.L., MA, Y.Q., WANG, Y.F., 2016c. *Improved flotation performance of hematite fines using citric acid as a dispersant*, Int. J. Miner. Metall. Mater., 23, 1119-1125.

OATS, W.J., OZDEMIR, O., NGUYEN, A.V., 2010. *Effect of mechanical and chemical clay removals by hydrocyclone and dispersants on coal flotation,* Miner. Eng., 23, 413-419.

PUGH, R.J., KITCHENER, J.A., 1971. *Theory of selective coagulation in mixed colloidal suspensions*, J. Colloid Interface Sci., 35, 656-664.

QIU, G.Z., HU, Y.H., WANG, D.Z., 1993. *Interaction between particles and fine particle flotation*, Central South University Press, China.

SCHENKEL, J.H., KITCHENER, J.A., 1960. *A test of the Derjaguin-Verwey-Overbeek theory with a colloidal suspension,* Trans. Faraday Soc., 56, 161-173.

SHAO, A.L., 2013. *Flotation separation of Donganshan carbonates-containing hematite ore*, J. Cent. South Univ., 44, 456-460.

SILVESTRE, M.O., PEREIRA, C.A., GALERY, R., PERES, A.E.C., 2009. *Dispersion effect on a lead-zinc sulphide ore flotation*, Miner. Eng., 22, 752-758.

VAN OSS, C. J., 2006. *Interfacial Forces in Aqueous Media*, Marcel Dekker, New York.

VAN OSS, C.J., CHAUDHURY, M.K., GOOD, R.J., 1987. *Monopolar surfaces*, Adv. Colloid Interface Sci., 28, 35-64.

VAN OSS, C.J., CHAUDHURY, M.K., GOOD, R.J., 1988. *Interfacial Lifshitz-van der Waals and polar interactions in macroscopic systems,* Chem. Rev., 88, 927-941.

VAN OSS, C.J., GOOD, R.J., 1989. *Surface tension and the solubility of polymers and biopolymers: the role of polar and apolar interfacial free energies*, J. Macromol. Sci., Pure Appl. Chem., 26, 1183-1203.

VAN OSS, C.J., GOOD, R.J., CHAUDHURY, M.K., 1987. *Determination off the hydrophobia interaction energy-application to separation processes,* Sep. Sci. Technol., 22, 1-24.

VAV OSS, C.J., GIESE, R.F., COSTANZO, P.M., 1990. *DLVO and non-DLVO interactions in hectorite*, Clays Clay Miner., 38, 151-159.

VERWEY, E.J., OVERBEEK, J.T.G., 1955. *Theory of the stability of lyophobic colloids*, J. Phys. Colloid Chem., 10, 224-225.

VIDELA, A.R., MORALES, R., SAINT-JEAN, T., GAETE, L., VARGAS, Y., MILLER, J.D., 2016. *Ultrasound treatment on tailings to enhance copper flotation recovery*, Miner. Eng., 99, 89-95.

WEI, R., PENG, Y.J., SEAMAN, D., 2013. *The interaction of lignosulfonate dispersants and grinding media in copper-gold flotation from a high clay ore*, Miner. Eng., 50-51, 93-98.

YANG, G., WANG, N.L., YIN, W.Z., LU, J.W., LUO, X.M., 2013. *Quality Improvement and Impurity Reduction Process Optimization of Donganshan Magnetic Coarse Concentrate with Dispersant NM-1*, Met. Mine., 9, 60-63.

YAO, J., HAN, H.L., HOU, Y., GONG, E.P., YIN, W.Z, 2016. *A Method of Calculating the Interaction Energy between Particles in Minerals Flotation*, Math. Probl. Eng., 1-13.

YIN, W.Z., HAN, Y.X., XIE, F., 2010. *Flotation Separation Research on Siderite-Containing Iron Concentrate*, Adv. Mater. Res., 103-109.

YIN, W.Z., LI, D., LUO, X.M., YAO, J., SUN, Q.Y., 2016. *Effect and mechanism of siderite on reverse flotation of hematite*, Int. J. Miner. Metall. Mater., 23, 373-379.

ZHANG, M., LIU, M.B., YIN, W.Z., HAN, Y.X., LI, Y.J., 2007. *Investigation on stepped-flotation process for Donganshan carbonate-containing refractory iron ore*, Met. Mine., 9, 62-64.

ZHANG, Z.Y., YIN, W.Z., LV, Z.F., HAN, Y.X., 2008. *Influence of the Siderite in Donganshan Iron Ore on Reverse Flotation*, Met. Mine., 10, 52-55.

ZHENG, X., SMITH, R.W., 1997. *Dolomite depressants in the flotation of apatite and collophane from dolomite*, Miner. Eng., 10, 537-545.

ZHU, J.J., YIN, W.Z., HOU, Y., WANG, N.L., YAO, J., WANG, Y.L., 2015. *Experimental study on dispersion flotation of Donganshan middling containing carbonate*, China Min. Mag., 24, 72-77.